

## THE SOURCE PARAMETERS OF THE SAN FERNANDO EARTHQUAKE INFERRED FROM TELESEISMIC BODY WAVES

BY MAX WYSS AND THOMAS C. HANKS

### ABSTRACT

The accuracy of teleseismic estimates of moment, fault area, dislocation and stress drop was tested for the case of a thrust fault: the San Fernando, California, earthquake of February 9, 1971. On the basis of  $P$ -wave spectra of 25 stations and  $S$ -wave spectra of 9 stations, the respective values were found to be  $0.7 \cdot 10^{26}$  dyne-cm,  $570 \text{ km}^2$ , 45 cm, and 14 bars. They agree well with the same parameters obtained from field observations. It is concluded that Brune's (1970) seismic source model is valid for the area determination of thrust earthquakes. The energy radiated in the form of  $S$  waves is estimated to be  $5 \cdot 10^{21}$  ergs.

### INTRODUCTION

For over a decade, theoretical seismologists have developed theories modeling earthquakes. These theories normally give the near- and far-field displacement spectra as a function of stress or displacement time functions at the source (Kasahara, 1957; Archambeau, 1968; Berckhemer and Jacob, 1968; Brune, 1970). As the source models of different theories vary, the predicted displacement spectra vary. Observational seismology has lagged behind by not checking empirically which of these theories, if any, correctly describes the far-field displacement spectra of earthquakes. Hanks and Wyss (1972) found that Brune's (1970) theory best estimates the source parameters of vertical strike-slip earthquakes. In this paper, the teleseismic body waves of the San Fernando, California, earthquake, which was a thrust event, are analyzed in detail. The source parameters, seismic moment, dimension, dislocation, and stress drop, derived from the seismic signals are compared to the same parameters estimated from the surface fracture and the aftershock zone. In addition, the seismic energy measured at teleseismic distances is compared to the energy measured in the near-field by Trifunac (1972) and the Gutenberg estimate.

The San Fernando, California, earthquake of February 9, 1971, provided an ideal opportunity to test source theories for thrust earthquakes. Since this event was located near the center of the seismic array of the California Institute of Technology, its hypocenter is known better than for most large local earthquakes (Allen *et al.*, 1971). The earthquake also produced a surface rupture, the displacements along which were mapped in detail by Kamb *et al.* (1971) and by Bonilla *et al.* (1971). Preliminary maps of the aftershock activity have been presented by Hanks *et al.* (1971) and Wesson *et al.* (1971). Fault-plane solutions were published by Whitcomb (1971) and Wesson *et al.* (1971).

### SOURCE PARAMETERS FROM FIELD DATA

The two parameters measured in the field are the rupture area  $A$  outlined by the aftershocks and surface trace, and the displacement  $\bar{u}$  across the surface faulting. The area outlined by the aftershock zone (corrected for the dip of the fault plane) was  $440 \text{ km}^2$  (Wesson *et al.*, 1971; Allen *et al.*, 1971; Hanks *et al.*, 1971). This area was roughly circular with a radius of  $r = 12 \text{ km}$ . It should be remembered that a secondary

plane of faulting has been tentatively identified by Hanks *et al.* (1971) and Whitcomb (1971), the Chatsworth segment. A group of shallow-focus earthquakes also do not fit into the simple picture of a single thrust plane (Hanks *et al.*, 1971). In spite of these complications, we will assume that the above-described fault area represents the dislocation surface of the main shock.

The displacement across the two main fault breaks differed considerably. The average displacement, two-thirds of the maximum, was 140 and 100 cm, respectively, on the western and eastern fault segment. For a thrust fault, the displacement at the free surface is expected to be magnified as much as a factor of 2 relative to the displacement at depth. For this reason, we take the smaller value, 100 cm, for the average displacement on the entire fault plane. It is possible that better estimates for the average displacement will become available when all geodetic observations are considered, and the uncertainty in the field-moment determination may be reduced.

Under the above assumptions we compute the seismic moment  $M_o$  from the field evidence (Aki, 1966).

$$M_o = \mu \bar{u} A \quad (1)$$

where  $\mu = 3 \cdot 10^{11}$  dyne/cm<sup>2</sup> is the shear modulus. The stress drop can be obtained from field data using Keilis-Borok's (1959) formula

$$\Delta\sigma = \pi \frac{\bar{u}}{r} \mu \frac{7}{16} \quad (2)$$

The estimates of these source parameters are given in Table 3.

#### TELESEISMIC OBSERVATIONS

The  $P$  waves recorded on the vertical components of 25 WWSSN stations (Table 1) at distances between 34° and 80° were Fourier analyzed. The resulting displacement spectra are shown in Figure 1. The long-period as well as the short-period recordings were used (*solid line* and *dots*, respectively, in Figure 1). In this way, the spectra are defined over as wide a frequency range as possible. This is necessary to determine the corner frequency  $f_o$  with confidence.

The  $S$ -wave spectra of nine stations are given in Figure 2. In order to avoid contamination of the  $S$  phase by other phases, only stations between 37° and 67° were analyzed. In an attempt to exclude  $S$ -coupled  $P$  waves from the analysis, stations with back azimuths close to  $n \cdot \pi/2$  degrees were preferentially used. In this case, the ray arrives at the station parallel to one and perpendicular to the other horizontal component. We then used the  $S$  wave recorded by the component approximately perpendicular to the ray, thus analyzing  $SH$  waves almost exclusively. The back azimuths and the components used are given in Table 2. All spectra presented in this paper have been corrected for instrument response and for attenuation using the results of Julian and Anderson (1968) for their earth model MM8.

Our basic teleseismic observations are body-wave spectra approximated in terms of two spectral parameters:  $\Omega_o$ , the long-period level, and  $f_o$ , the corner or peak frequency. A general feature of all dislocation models is that  $\Omega_o$  is proportional to  $M_o$  (Keilis-Borok, 1959; Maruyama, 1963; Burridge and Knopoff, 1964; Ben-Menahem and Harkrider, 1964; Ben-Menahem *et al.*, 1965; Aki, 1966), and  $f_o$  is proportional to the reciprocal of the source dimension  $r$  (Jeffreys, 1931; Kasahara, 1957; Archambeau, 1968; Berckhemer and Jacob, 1968; Brune, 1970). Assuming that the ruptured area was circular, we can infer  $D$  and  $\Delta\sigma$  from  $M_o$  and  $r$ . In addition, the seismic energy radiated in  $P$  and  $S$  waves can be obtained.

The method of estimating the source parameters from teleseismic data is that described by Hanks and Wyss (1972). The spectra shown in Figures 1 and 2 were fitted by an approximate long-period constant level  $\Omega_0$  and an average straight line through the short-period decaying part of the spectrum. For the  $P$  waves the short-period data decayed on the average as  $f^{-1.8}$  and for the  $S$  waves as  $f^{-1.5}$ . The rate of decay is given for each spectrum in Tables 1 and 2 as  $\gamma$ , and it will be discussed further in the section considering stress drop. The corner frequency  $f_0$  is defined as the intersection of the two straight-line approximations of the long- and short-period part of the spectrum.

TABLE 1  
P-WAVE SPECTRAL CHARACTERISTICS—February 9, 1971

Station	Distance (deg)	Azimuth (deg)	$\Omega_0$ $10^{-2}$ cm/sec	$f_0$ (Hz)	$\gamma$	$M_0^*$ ( $10^{26}$ dyne-cm)	$M_0^\dagger$
NOR	57.9	9.8	0.5	0.17	2.2	0.48	0.95
KEV	73.1	11.9	0.4	0.11	1.5	0.64	1.15
UME	76.8	17.5	0.17	0.14	1.8	0.21	0.36
NUR	80.7	17.5	0.37	0.13	1.2	0.33	0.53
KTG	60.1	22.7	0.45	0.17	2.0	0.41	0.71
GDH	49.4	25.1	0.72	0.15	2.0	0.80	1.47
COP	81.0	25.7	0.3	0.16	1.6	0.27	0.41
STU	85.0	31.7	0.2	0.14	2.0	0.23	0.33
ESK	74.9	32.4	0.23	0.15	2.0	0.28	0.40
VAL	73.6	37.8	0.48	0.15	2.1	0.56	0.77
PTO	81.0	46.0	0.4	0.15	2.0	0.32	0.42
WES	37.4	63.4	0.57	0.08	—	0.49	0.50
OGD	35.0	65.9	0.34	0.07	1.3	0.27	0.26
GEO	33.3	70.0	0.8	0.065	1.7	0.68	0.64
BEC	44.5	76.9	0.4	0.12	—	0.38	0.38
SJG	49.1	95.5	0.36	0.12	—	0.23	0.23
TRN	56.9	100.3	0.3	0.14	2.0	0.23	0.22
CAR	52.5	104.2	0.4	0.13	1.5	0.31	0.31
LPB	69.7	128.1	0.45	0.11	—	0.30	0.32
ARE	67.4	130.6	0.4	0.16	1.8	0.28	0.30
AFI	69.8	236.1	0.4	0.12	2.2	0.38	0.62
KIP	37.1	260.1	0.52	0.2	1.5	0.40	0.82
GUA	87.9	284.9	0.23	0.3	1.8	0.26	0.44
MAT	79.6	307.2	0.28	$\geq 0.16$	—	0.32	0.60
COL	35.3	338.8	0.4	0.12	2.1	0.40	2.03

\* Fault-plane solution by Whitcomb (1971)

† Fault-plane solution by Wesson *et al.* (1971)

For the estimate of moment and radiated energy, the following corrections of the displacement spectral amplitudes were made. For the combined displacement amplification by the free surface and the crust at the receiver, an average value of the transfer functions found by Ben-Menahem *et al.* (1965) was assumed to be 2.5 and applied to all frequencies of  $P$  and  $S$  waves. Corrections for the radiation patterns by Whitcomb (1971) and Wesson *et al.* (1971) were made. The decrease in amplitude due to geometrical spreading was accounted for using the results of Julian and Anderson (1968). The spatial integration of the radiated energy was performed applying Wu's (1966) results to a half-space.

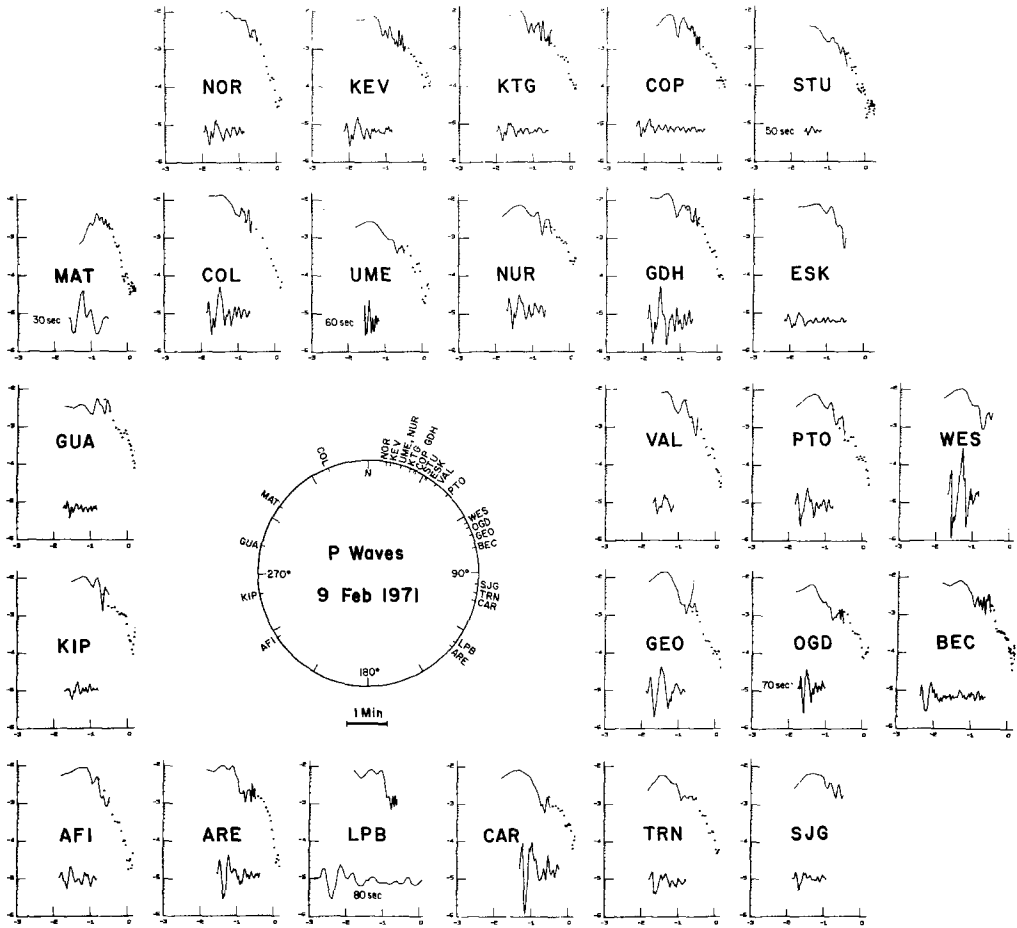


FIG. 1. *P*-wave displacement spectra of the San Fernando earthquake arranged as a function of azimuth. On the ordinate, the log of ground motion (displacement spectral density) is plotted in units of 1.76 cm sec. The abscissa gives log of frequency in Hertz. Long-period instrument given by *solid line*, short period by *points*. The *traces* shown are the long-period signals for which the length of a minute is shown near the center. For five signals the time scale was different. In these cases, the total signal length in seconds is given next to the signals.

## DISCUSSION

*Seismic moment.* Assuming that the long-period level is constant to infinitely long periods, we estimate the seismic moment through the relation (Keilis-Borok, 1959; Ben-Menahem *et al.*, 1965)

$$M_o = 4\pi\rho v^3 \Delta \frac{\Omega_o}{R_{\theta\phi}} \quad (3)$$

where  $\rho$  = density at the source,  $v$  = wave velocity of the appropriate phase at the source,  $\Delta$  = term accounting for geometrical spreading in a spherical Earth, and  $R_{\theta\phi}$  = radiation pattern.  $M_o$  for each station is given in Tables 1 and 2.

For a shallow source in a realistic Earth, teleseismic stations sample only a small range of body-wave ray directions. For the body waves considered here, the take-off angles of the rays (measured from the vertical) varied only between  $15^\circ$  and  $29^\circ$ . Since the main thrust plane dipped at an angle near  $45^\circ$ , this implies that *P* waves recorded at teleseismic distances will be near a maximum in the radiation pattern and *S* waves will

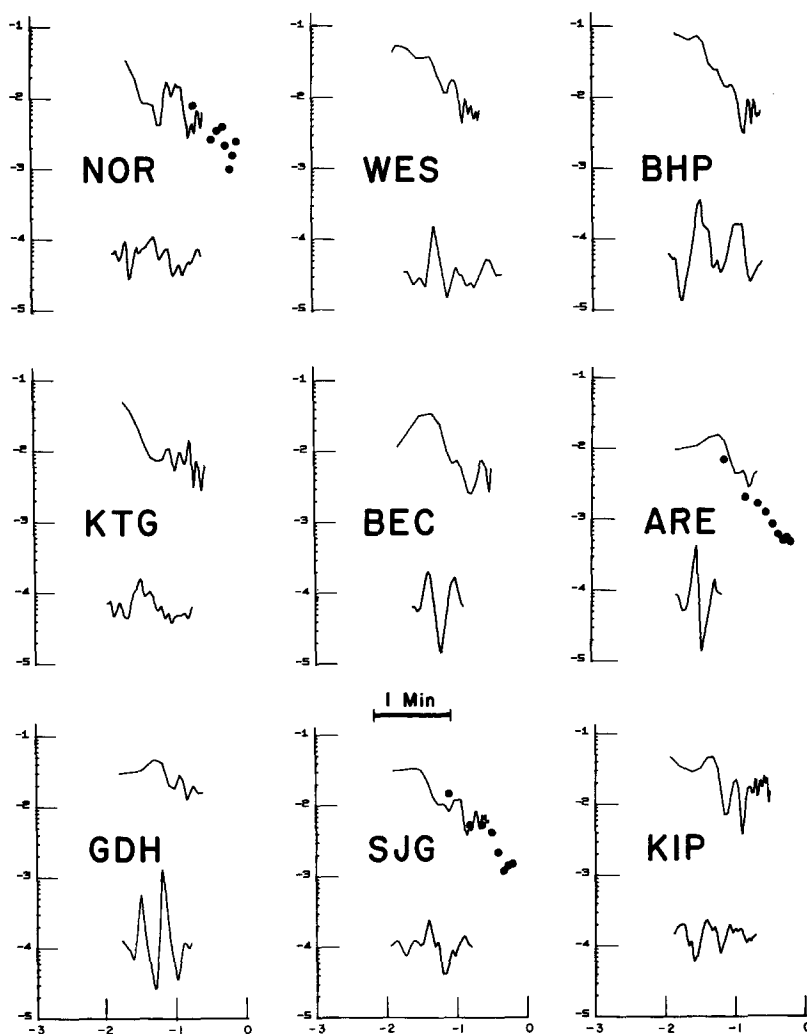
FIG. 2. *S*-wave spectra of the San Fernando earthquake of February 9, 1971 (see Figure 1).

TABLE 2

*S*-WAVE SPECTRAL CHARACTERISTICS, February 9, 1971

Station and Component	Distance (deg)	Back Azimuth (deg)	Azimuth (deg)	$\Omega_0$ ( $10^{-2}$ cm/sec)	$f_0$ (Hz)	$\gamma$	$M_0^*$ ( $10^{26}$ dyne-cm)	$M_0^\dagger$
NOR N	57.9	287.1	9.8	0.63	0.17	1.2	—	0.33
KTG N	60.1	288.6	22.7	0.5	$\geq 0.2$	—	—	0.26
GDH N	49.4	260.3	25.1	2.2	0.08–0.16	—	—	0.59
WES N	37.4	273.6	63.4	2.8	0.045	—	0.47	0.30
BEC N	44.5	287.9	76.9	1.7	0.07	1.6	0.31	0.23
SJG N	49.1	300.1	95.5	1.9	0.04–0.06	1.5	0.36	0.34
BHP E	43.7	311.3	116.2	4.0	0.04	—	1.11	1.85
ARE N	67.4	319.2	130.6	0.8	0.09	1.8	0.75	—
KIP N	37.1	61.0	260.1	2.3	0.06–0.1	—	—	1.7

\* Fault-plane solution by Whitcomb (1971)

† Fault-plane solution by Wesson *et al.* (1971)

be near a node. For a vertical strike-slip fault, the converse is true. Hanks and Wyss (1972) found that near-nodal  $P$ -wave amplitudes for three large vertical strike-slip earthquakes were often considerably larger than would be expected from the point-source radiation pattern. For the San Fernando earthquake-source geometry, we then expect that  $P$ -wave moments will be more reliable than  $S$ -wave moments.

Two moment determinations for each station are given in Tables 1 and 2, based on the fault-plane solutions by Whitcomb (1971) and Wesson *et al.* (1971). The average moment based on  $P$  waves is  $0.38 \pm 0.15 \cdot 10^{26}$  dyne-cm and  $0.55 \pm 0.28 \cdot 10^{26}$  dyne-cm, respectively. The average  $S$ -wave moment is  $0.63 \cdot 10^{26}$  dyne-cm and  $1.14 \cdot 10^{26}$  dyne-cm, respectively. Since the two rms errors are not significantly different percentage-wise, we have no preference with respect to the fault-plane solution, and we take the average of the two respective moment values as the moment determined from teleseismic body-waves,

$$M_o(P) = 0.47 \cdot 10^{26} \text{ dyne-cm, and } M_o(S) = 0.88 \cdot 10^{26} \text{ dyne-cm.}$$

TABLE 3  
SOURCE PARAMETERS, February 9, 1971

	Moment $M_o$ ( $10^{26}$ dyne-cm)	Length, $L = 2r$ (km)	Area, $\pi r^2$ ( $\text{km}^2$ )	Dislocation, $\bar{u}$ (cm)	Stress, Drop, $\Delta\sigma$ (bar)
Field evidence	1.3	24	440	100	34
$P$ wave (Brune, 1970)	0.47	30	708	22	6
$S$ wave (Brune, 1970)	0.88	24	440	67	21
$P$ wave (Berckhemer and Jacob, 1968)	0.47	10	73	215	165
$P$ wave (Kasahara)	0.47	9	70	224	198
Surface waves (Aki, personal communication)	0.75	—	—	—	—

In Table 3, the several estimates of  $M_o$  are compared. The agreement between the average moment determinations based on  $P$  waves,  $S$  waves and surface waves (Aki, personal communication) is excellent. The  $P$ -wave and  $S$ -wave results may be expected to overestimate the moment because the surface reflections  $pP$  and  $sS$  could not be excluded in the analysis; the static moment, however, is larger. The accuracy of a static moment determination was estimated to be between a factor of 3 and 5 (Hanks and Wyss, 1972). The largest part of this uncertainty is connected with the estimate of the average displacement. If the latter can be improved, the check on the body-wave moments will be improved, and it may turn out that their accuracy is greater than what we are able to claim now. The teleseismic and static moments given in Table 3 agree with each other within a factor less than 3. We conclude that the moment of a thrust fault can reliably be determined from teleseismic observations.

*Source dimensions and rupture velocity.* Several authors have proposed equations relating the corner or peak frequency  $f_o$  of the seismic spectrum to the source dimension (e.g., Kasahara, 1957; Berckhemer and Jacob, 1968; Brune, 1970). In the test case of the Borrego Mountain, California, earthquake which produced a well-documented surface rupture and aftershock zone (Allen *et al.*, 1968; Hamilton, 1971), it was found (Hanks and Wyss, 1972) that the theory by Brune (1970) best predicted the source dimensions  $r$  from body-wave spectra. Brune's (1970) relation between corner frequency  $f_o$  and the source area  $A$  is

$$A = \frac{1.17^2 v^2}{\pi f_o^2} \quad \text{or} \quad r = \frac{1.17v}{\pi f_o} \quad (4)$$

where  $v$  is the  $S$ -wave velocity. Wyss *et al.* (1971) and Hanks and Wyss (1972) proposed that equation (4) may be extended to  $P$  waves by using the  $P$ -wave velocity for  $v$ . Their rationale was that the critical wavelength  $\lambda_o$  corresponding to  $f_o$  had to be held constant in equation (4) since the corner in the spectrum was due to interference of waves with wavelengths longer than the source dimension. It should be remembered, however, that (4) for  $P$  waves lacks a theoretical justification. While future theoretical studies may improve the relation (4) for  $P$  waves, we intend to establish its approximate validity empirically for thrust earthquakes in this paper.

Berckhemer and Jacob (1968) give the following relation for  $P$  waves

$$A = \frac{c_{\max}^2}{2\pi f_o^2} \quad (5)$$

where  $\pi r^2 = A$ , and where  $c_{\max}$  is the maximum propagation velocity, which was assumed here to be 3 km/sec. Trifunac (1972) estimated the average rupture velocity to be approximately 2 km/sec.

Kasahara (1957) gives the following relation for  $P$  waves

$$r = \frac{0.66}{f_o(P)} \quad (6)$$

Values of  $f_o(P)$  and  $f_o(S)$  are given in Tables 1 and 2, respectively. Generally, the high-frequency spectral decay (and  $f_o$ ) was only well-defined when the short-period data were available. For this reason, we consider  $f_o(P)$  to be somewhat more reliable than  $f_o(S)$ . The average corner frequency was found to be  $f_o(P) = 0.14$  Hz for  $P$  waves and  $f_o(S) = 0.1$  Hz for  $S$  waves. The corresponding circular source area  $A$  of radius  $r$  and source length  $L = 2r$  were computed from all of the above equations.

These source dimensions are compared to the field observations in Table 3. The fault area and length estimate based on body-wave analysis using Brune's (1970) equation is in good agreement with the field evidence, whereas the earlier equations (5) and (6) underestimate the source size.

The corner frequency and, hence, the inferred source dimension shows a marked azimuthal dependence (Figure 3). This fact together with the lack of enough short-period data and an error in the Fourier analysis program led to an underestimate for  $f_o$  (overestimate for  $r$ ) and an overestimate for  $M_o$  in the preliminary analysis of the source parameters of the San Fernando earthquake (Wyss, 1971).

In Figure 3, a group of stations due ENE have low corner frequencies and stations due west show high corner frequencies. This observation could be explained by a propagating source if the azimuths of the two groups of stations were different by  $180^\circ$ , since a propagating source will modulate the radiation pattern by focusing energy in the forward direction of propagation at the expense of azimuths in the backward direction (Ben-Menahem, 1961). Considering the complicated surface fracture with thrust on the eastern and strike-slip on the western fault segment, one could postulate that the propagation of rupture might have been parallel to either slip direction at different times during the rupture process. With such an assumption the distribution of  $f_o$  values in Figure 3 might be explained. Further, by inspection of the  $\sin \chi/\chi$  function (Ben Menahem, 1961), one can see that the data in Figure 3 are consistent with a rupture propagating from ENE to W with a velocity of approximately 2.5 km/sec.

The data and method of analysis are not sufficient to allow a more detailed estimate of rupture speed and direction particularly because not only  $P$  but  $pP$  is contained in our data sample, and correction for crustal reverberations near the stations could not be

made. However, we feel that the effect on the spectra is quite real. In Figure 1, it can be seen that the eastern spectra with the low corner frequencies have also a very pronounced minimum near the corner frequency in accordance with the  $\sin \chi/\chi$  modulation. In this respect the eastern and western spectra look very different. Our crude estimate of rupture speed is also in agreement with the result of Trifunac (1972) who gives 2 km/sec.

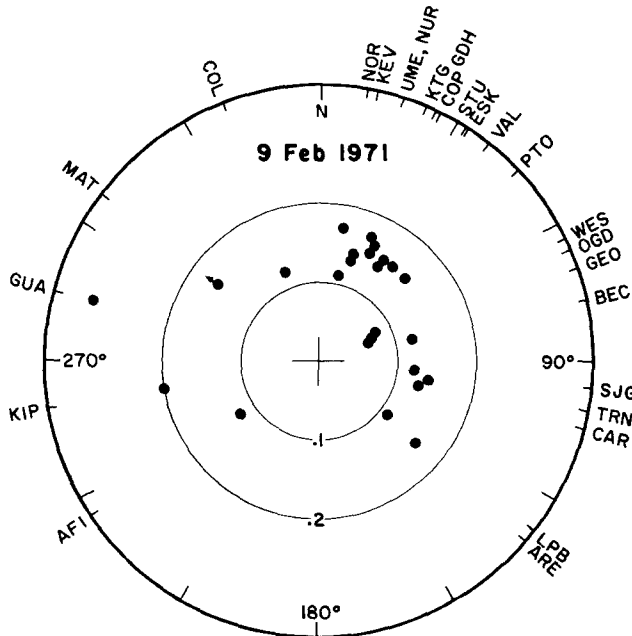


FIG. 3. Corner frequency (Hz) plotted as a function of azimuth. Arrow indicates minimum estimate.

*Dislocation.* From the moment and rupture area obtained by body-wave analysis, the average dislocation across the fault plane can be estimated using equation (1). The accuracy of the dislocation estimate from body waves is less than the accuracy with which the basic parameters, moment and area, are obtained. As a consequence, the agreement between the different methods is only fair, (Table 3). The results based on Brune's (1970) and Berckhmer and Jacob's (1968) results bracket the field measurement about evenly on the low and high side.

*Stress drop.* The stress drop is the difference between the shear stress on the fault surface before and after the rupture  $\Delta\sigma = \sigma_1 - \sigma_2$ . Since we wish to test the teleseismic method to obtain  $\Delta\sigma$ , we assume a circular source as we would in the case of unknown source geometry, and we use the relation (Brune, 1970)

$$\Delta\sigma = \frac{7}{16} \frac{M_0}{r^3}. \quad (7)$$

The comparison in Table 3 again shows that the agreement between Brune's (1970) model and the field evidence is good. Weighting the body-wave and field data equally, the average stress drop is 24 bars. This value is small compared to the result of Trifunac (1972) who found from a near-field strong-motion record that the effective stress  $\sigma_{\text{eff}}$  (Brune, 1970) was 100 bars for the San Fernando earthquake. The effective stress was defined by Brune as the difference between the initial stress and the average frictional stress during the rupture. In this terminology, complete stress drop is considered to have

taken place if the final stress equals the frictional stress. A comparison of  $\Delta\sigma$  with  $\sigma_{\text{eff}}$  shows that in the case of the San Fernando earthquake only a fractional stress drop of approximately 20 per cent occurred.

Since the effective stress  $\sigma_1 - \sigma_f$  is larger than the stress drop  $\sigma_1 - \sigma_2$ , it follows that  $\sigma_2 > \sigma_f$ . This result does not conform to the frictional fault models suggested by Orowan (1960) and Savage and Wood (1972) for which  $\sigma_f \geq \sigma_2$ . While the sources of error in the stress drop and effective stress determinations are such that the stress drop *could* be larger than the effective stress, the estimates given above are still the most reliable determinations of both quantities for a single earthquake that are presently available. A more serious difficulty is that both quantities are defined only in an average sense. Whether  $\sigma_2 > \sigma_f$  at every point on the fault surface cannot be decided with the method used.

In the Brune (1970) model of the seismic source, small  $\varepsilon = \Delta\sigma/\sigma_{\text{eff}}$  manifests itself in the *S*-wave spectrum by requiring  $f^{-1}$  falloff of the spectrum in the frequency range  $f_o(S) \leq f \leq f_o(S)/\varepsilon$ . For  $\varepsilon = 0.2$  and  $f_o(S) = 0.1$  Hz, the *S*-wave spectra should then fall off as  $f^{-1}$  in the frequency range  $0.1 \leq f \leq 0.5$ . Most of the *S*- and *P*-wave spectra in Figures 1 and 2 would lend themselves to an interpretation in terms of an  $f^{-1}$  initial falloff. We feel, however, that the modulations by crustal transfer functions and other effects do not warrant such a detailed interpretation. Rather than attempt a possibly subjective interpretation in terms of fixed slopes, we have fitted an average line through the spectra and given the slope of decay as  $\gamma$  in Tables 1 and 2. The average slope of all well-defined *S*-wave spectra was 1.5 and for *P* waves it was 1.8. The fact that these slopes are less than two is a qualitative indication for partial stress drop, if Brune's (1970) model is accepted as correct.

The low stress drop of the San Fernando earthquake is not surprising. It is comparable to those for other earthquakes of similar magnitude whose stress drops are well known, as in the case of the Imperial (Brune and Allen, 1968), the Parkfield (Aki, 1967; Wyss and Brune, 1968), the Borrego Mountain (Wyss and Hanks, 1972), and the Denver (Wyss and Molnar, 1972) earthquakes. In these cases, the stress drops were 1, 7, 9, and 5 bars, respectively.

*Estimates of radiated energy.* The energy radiated in the form of the *S* wave,  $E_s$ , whose spectrum is given by the Brune (1970) model with  $\varepsilon$  arbitrary, is approximately

$$E_s \simeq \frac{96\pi^3}{15} \rho \beta \Delta^2 \Omega_o^2(S) f_o^3(S) \left[ \frac{2}{\varepsilon} - \frac{2}{3} \right] \quad (8)$$

(see Hanks and Wyss, (1972) for a derivation of this result). A similar relation for the energy radiated in the form of *P* waves demonstrates that it is small compared to the *S*-wave energy (Wu, 1966).

Figure 4 is an inferred composite *S*-wave spectrum for the San Fernando earthquake at Pasadena. The long-period level is based on the teleseismic observations reduced to the distance of 45 km as it should have appeared had instruments over the appropriate frequency range been on scale. In fact, the only unsaturated instrument was the very low-gain ( $4 \times$ ) Wood-Anderson (NS) torsion seismograph which supplied usable spectral data over the range  $0.5 < f < 2.5$  Hz (*solid line* in Figure 4). These spectral data are a useful consistency check on the same data obtained at teleseismic distances.

The horizontal dashed line represents  $\Omega_o/R_{\theta\phi}$ , obtained from the average value of  $M_o(S)$  using (3). Its high-frequency terminus is the average determination of  $f_o(S)$ , 0.1 Hz. The sloping dashed lines in Figure 4 represent the cases  $\varepsilon = 1$  and  $\varepsilon = 0.2$  approximated from Brune (1970). The short-period data are intermediate with respect

to the two cases. Since we have chosen average values for  $\Omega_0/R_{\theta\phi}$  and  $f_0(S)$ , it is possible that their actual values at Pasadena could be such to admit any value of  $\epsilon$  between 0.2 and 1. If we then assume that an equal amount of energy was contained in the EW motion, we obtain by (8) for the energy in the SH waves a minimum value of  $\sim 1 \cdot 10^{21}$  ergs for  $\epsilon = 1$  and a maximum value of  $8 \cdot 10^{21}$  ergs for  $\epsilon = 0.2$ .

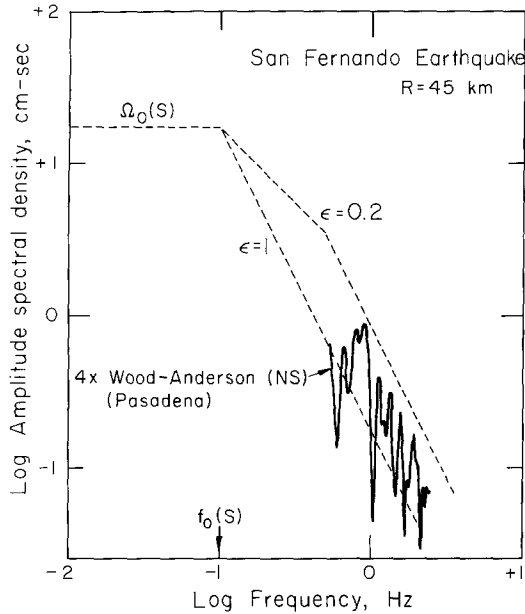


FIG. 4. *S*-wave spectrum of the San Fernando earthquake recorded at Pasadena by Wood-Anderson (NS), extrapolated to low frequencies on the basis of the teleseismic spectra.

The Gutenberg-Richter estimate of radiated energy  $E_{GR}$  can be obtained from

$$\log E_{GR} = 9.9 + 1.9M_L - 0.024M_L^2 \quad \text{Richter (1958)}$$

where  $M_L$  is the local magnitude (Richter, 1958) = 6.6 for the San Fernando earthquake. Then  $E_{GR} = 2.5 \times 10^{21}$  ergs, very close to the  $\epsilon = 1$  estimate for  $E_s$ . Trifunac (1972) estimated the total *S*-wave energy (including *SV*) to be  $1.7 \cdot 10^{22}$  ergs from a near-field acceleration record (Pacoima Dam). This agrees more closely with our  $\epsilon = 0.2$  estimate for  $E_s$ . Given the uncertainties in any estimate, the various estimates agree well. We consider the seismically-radiated energy of the San Fernando earthquake to be relatively well-determined, its value being in the range  $10^{21.3}$  to  $10^{22.3}$  ergs.

### CONCLUSIONS

Spectral analysis of 25 *P*-wave and nine *S*-wave recordings of the San Fernando, California, earthquake at a wide range of azimuths and distances ( $33^\circ$  to  $88^\circ$ ) showed that the dimensions of a thrust earthquake can be estimated successfully using Brune's (1970) source theory. It was also demonstrated that the seismic moment of a thrust earthquake can be estimated as well from spectral analysis of teleseismic body-wave signals as from field observations in the case of a surface rupture. It follows that the dislocation at the source and the stress drop can be extracted within a factor of approximately 3 to 5 from teleseismic observations.

Considering field and spectral data, the seismic moment of the San Fernando earthquake was approximately  $1 \cdot 10^{26}$  dyne-cm, and the stress drop was approximately 20 bars, only about 20 per cent of the effective stress.

The estimate of total radiated seismic energy from far-field recordings is approximately  $5 \cdot 10^{21}$  ergs which agrees reasonably well with near-field data and the Gutenberg-Richter estimate.

#### ACKNOWLEDGMENTS

We thank Mr. Modgling of the Environmental Data Service, NOAA for furnishing the data from the WWSSN speedily, and we wish to thank Miss C. Schreiber for digitizing the records. We also are grateful to J. Savage, K. Jacob, and M. Trifunac for reading the manuscript critically and making many helpful suggestions. This study was supported by USGS Contract No. 14-08-0001-12289, and National Science Foundation Grant NSF GA-29920.

#### REFERENCES

- Aki, K. (1966). Generation and propagation of *G*-waves from the Niigata earthquake of June 16, 1964: Part 2. Estimation of earthquake moment, released energy, and stress-strain drop from the *G*-wave spectrum, *Bull. Earthquake Res. Inst., Tokyo Univ.* **44**, 73-88.
- Aki, K. (1967). Scaling law of seismic spectrum, *J. Geophys. Res.* **72**, 1217-1231.
- Allen, C. R., G. R. Engen, T. C. Hanks, J. M. Nordquist, and W. R. Thatcher (1971). Main shock and larger aftershocks of the San Fernando earthquake February 9 through March 1, 1971, *U.S. Geol. Surv. Profess. Paper* 733, 17-20.
- Allen, C. R., A. Grantz, J. N. Brune, M. M. Clark, R. V. Sharp, T. G. Theodore, E. W. Wolfe, and M. Wyss (1968). The Borrego Mountain, California, earthquake of 9 April 1968: A preliminary report, *Bull. Seism. Soc. Am.* **58**, 1183.
- Archambeau, C. B. (1968). General theory of elastodynamic source fields, *Rev. Geophys.* **6**, 241-288.
- Ben-Menahem, A. (1961). Radiation of seismic surface waves from finite moving sources, *Bull. Seism. Soc. Am.* **51**, 401-435.
- Ben-Menahem, A. and D. Harkrider (1964). Radiation patterns of seismic surface waves from buried dipolar point sources in a flat stratified earth, *J. Geophys. Res.* **69**, 2605-2620.
- Ben-Menahem, A., S. W. Smith, and Ta-Liang Teng (1965). A procedure for source studies from spectrums of long-period seismic body waves, *Bull. Seism. Soc. Am.* **55**, 203-235.
- Berckhemer, H. and K. H. Jacob (1968). Investigation of the dynamical process in earthquake foci by analysing the pulse shape of body waves, *Final Scientific Report, AF 61(052)-801*, Air Force Cambridge Research Laboratories.
- Bonilla, M. G., J. M. Buchanan, R. O. Castle, M. M. Clark, V. A. Frizzell, R. M. Gulliver, F. K. Miller, J. P. Pinkerton, D. C. Ross, R. V. Sharp, R. F. Yerkes, and J. F. Ziouy (1971). Surface faulting (in the San Fernando, California, earthquake of February 9, 1971), *U.S. Geol. Surv. Profess. Paper* 733, 55-76.
- Brune, J. N. (1970). Tectonic stress and the spectra of seismic shear waves from earthquakes, *J. Geophys. Res.* **75**, 4997-5009.
- Brune, J. N. and C. R. Allen (1967). A low stress-drop, low-magnitude earthquake with surface faulting The Imperial, California, earthquake of March 4, 1966, *Bull. Seism. Soc. Am.* **57**, 501-514.
- Burridge, R. and L. Knopoff (1964). Body force equivalents for seismic dislocations, *Bull. Seism. Soc. Am.* **54**, 1874-1888.
- Hamilton, R. (1971). Aftershocks of the Borrego Mountain, California, earthquake from April 12 to June 12, 1968, *U.S. Geol. Surv. Profess. Paper*, (in preparation).
- Hanks, T. C., T. H. Jordan, and J. B. Minster (1971). Precise locations of aftershocks of the San Fernando earthquake 2300 (GMT) February 10-1700 February 11, 1971, *U.S. Geol. Surv. Profess. Paper* 733, 21-23.
- Hanks, T. C. and M. Wyss (1972). The use of body wave spectra in the determination of seismic source parameters, *Bull. Seism. Soc. Am.* **62**, 561-589.
- Jeffreys, H. (1931). On the cause of oscillatory movement in seismograms. *Monthly Notices Roy. Astron. Soc. Geophys. Suppl.* **2**, 407-441.

- Julian, B. R. and D. L. Anderson (1968). Travel times, apparent velocities and amplitudes of body waves, *Bull. Seism. Soc. Am.* **58**, 339-366.
- Kamb, B., L. T. Silver, M. J. Abrams, B. A. Carter, T. H. Jordan, and J. B. Minster (1971). Pattern of faulting and nature of fault movement in the San Fernando earthquake, *U.S. Geol. Surv. Profess. Paper 733*, 41-54.
- Kasahara, K. (1957). The nature of seismic origins as inferred from seismological and geodetic observations, *Bull. Earthquake Res. Inst., Tokyo Univ.* **35**, 473-532.
- Keylis-Borok, V. I. (1959). An estimation of the displacement in an earthquake source and of source dimensions, *Ann. Geofis. (Rome)* **12**, 205-214.
- Maruyama, T. (1963). On the force equivalent of dynamic elastic dislocations with reference to the earthquake mechanism, *Bull. Earthquake Res. Inst., Tokyo Univ.* **41**, 464-486.
- Orowan, E. (1960). Mechanism of seismic faulting, Rock Deformation, a symposium, D. Griggs and T. Handin, Editors, *Geol. Soc. Am., Mem. 79*, 323-345.
- Richter, C. F. (1958). *Elementary Seismology*, W. H. Freeman & Co, San Francisco.
- Savage, J. C. and M. D. Wood (1971). The relation between apparent stress and stress drop, *Bull. Seism. Soc. Am.* **61**, 1381-1388.
- Trifunac, M. D. (1972). Stress estimates for the San Fernando, California, earthquake of February 9, 1971 (in preparation).
- Wesson, R. L., W. H. K. Lee, and J. F. Gibbs (1971). Aftershocks of the earthquake (in The San Fernando, California, Earthquake of 9 February 1971), *U.S. Geol. Surv. Profess. Paper 733*, 24-29.
- Whitcomb, J. H. (1971). Fault plane solutions of the February 9, 1971 San Fernando earthquake and some aftershocks, *U.S. Geol. Surv. Profess. Paper 733*, 30-32.
- Wu, F. T. (1966). Lower limit of the total energy of earthquakes and partitioning of energy among seismic waves, *Ph.D. Thesis*, California Institute of Technology.
- Wyss, M. (1971). Preliminary source parameter determination of the San Fernando earthquake, *U.S. Geol. Surv. Profess. Paper 733*, 38-40.
- Wyss, M. and J. N. Brune (1968). Seismic moment, stress and source dimensions for earthquakes in the California-Nevada region, *J. Geophys. Res.* **73**, 4681-4694.
- Wyss, M. and T. C. Hanks (1972). The source parameters of the Borrego Mountain, California, earthquake, *U.S. Geol. Surv. Profess. Paper* (in press).
- Wyss, M., T. C. Hanks and R. C. Liebermann (1971). Comparison of *P*-wave spectra of nuclear explosions and earthquakes, *J. Geophys. Res.* **76**, 2716-2729.
- Wyss, M. and P. Molnar (1972). Efficiency, stress-drop, apparent stress, effective stress and frictional stress of Denver, Colorado, earthquakes, *J. Geophys. Res.* **77**, 1433-1438.

LAMONT-DOHERTY GEOLOGICAL OBSERVATORY  
OF COLUMBIA UNIVERSITY  
PALISADES, NEW YORK 10964 (M.W.)  
CONTRIBUTION NO. 1753

SEISMOLOGICAL LABORATORY  
CALIFORNIA INSTITUTE OF TECHNOLOGY  
PASADENA, CALIFORNIA 91109 (T.C.H.)  
CONTRIBUTION NO. 2064, DIVISION OF  
GEOLOGICAL SCIENCES

Manuscript received July 14, 1971